

Original Article

Design of Wearable Patch Antenna for X-band Applications

G. Prema¹, G. Shobana¹, V. Gnanalakshmi^{1*}

¹Department of Electronics and Communication Engineering, MepcoSchlenk Engineering College, Sivakasi, India.

*Corresponding Author : v.gnanalakshmi@mepcoeng.ac.in

Received: 12 March 2025

Revised: 15 April 2025

Accepted: 16 May 2025

Published: 27 May 2025

Abstract - This paper presents a wearable microstrip line-fed rectangular patch antenna (WLF_MPA) using a denim substrate designed for X-band applications centered at 8.91 GHz. The antenna operates within a frequency range of 8.72 GHz to 9.09 GHz, offering a radiation efficiency of 70% and a gain of 6.4 dB. The Specific Absorption Rate (SAR) for 1g muscle mass is 0.8912 W/Kg, well within the standard safety limit of 1.6 W/Kg. Using denim as a flexible substrate ensures comfort and durability for wearable applications. These characteristics make the antenna ideal for X-band applications such as industrial monitoring, healthcare, and defense communications.

Keywords - Wearable antenna, Microstrip patch, X-band, Denim, SAR.

1. Introduction

Wearable devices are gaining increasing attention across various fields, including medical diagnostics, health and fitness monitoring, industrial safety, and defense systems. However, designing wearable antennas presents significant challenges, primarily due to their close proximity to the human body.

This interaction can cause undesirable electromagnetic coupling, resulting in frequency detuning, reduced radiation efficiency, and increased power absorption by body tissues. These effects degrade antenna performance and may raise health concerns due to long-term exposure to electromagnetic radiation [1]. The key research gap lies in the need for a compact, efficient, and safe antenna design that maintains stable performance when in contact with the human body, particularly at higher frequency bands such as the X-band (8-12 GHz). Although several studies have addressed antenna miniaturization and material selection, limited work has focused on optimizing antenna performance specifically for the X-band while ensuring compliance with Specific Absorption Rate (SAR) limits set by regulatory bodies like the American National Standards Institute (ANSI) as 1.6 W/kg and ICNIRP as 2 W/kg [2].

Moreover, most existing designs either suffer from bulky structures or utilize non-durable or costly materials, limiting their practicality in daily wearable applications. Hence, this work's primary problem is designing a low-profile, cost-effective, and SAR-compliant wearable antenna that can operate efficiently in the X-band without performance degradation due to body interaction.

The main objectives of the paper are:

- To design and analyze a WLF_MPA antenna using a denim substrate operating in X-band centered at 8.91 GHz.
- Characterize its performance through simulations, such as return loss, VSWR, gain, directivity, and radiation efficiency.
- To simulate a human phantom model to verify that the antenna complies with SAR safety restrictions for wearable applications.
- To compare the proposed design with existing wearable antenna models, highlighting its advantages in performance and cost-effectiveness.

In this work, a denim-based wearable antenna-fed by a coplanar waveguide and featuring a rectangular radiating patch has been developed for operation at 8.91 GHz (X-band), with a measured bandwidth of 0.31 MHz ($\epsilon_r = 1.70$). Electromagnetic simulations were performed using ANSYS HFSS R2021. Section II includes a literature survey. Section III covers the antenna geometry and substrate properties, Section IV presents the simulation outcomes, and Section V offers concluding remarks.

2. Literature Survey

Textile antennas often use substrates such as felt, denim, Kevlar, fleece fabrics, cotton, polyester, cordura, lycra, and conductive textiles as patches. It is crucial that the antenna's efficiency remains unaffected when mounted on the human body [1-3]. A tri-band coplanar waveguide-fed patch antenna has been proposed to reduce the backward radiation. An



Artificial Magnetic Conductor with Graphene Assembled Film substrate and a 3 x 3 array where each unit cell contains three circular patches to work on three different bands is used [2]. A microstrip-fed antenna with a rectangular patch was designed on a jeans substrate with a relative permittivity of 1.7 and a loss tangent of 0.025, and it is proposed for Wireless Body Area Networks (WBAN) applications [4]. A Substrate Integrated Waveguide (SIW) textile antenna is proposed where three metallic vias connect the ground plane with the substrate and patch, and the circular polarization is realized by using SIW holes at two bands [5]. Different modes can be fed with different frequencies by adaptive patch loading and reconfiguring the feed structure. This antenna consists of straight and inverted “T” shaped branches integrated onto a rectangular patch, a full grounding plane and a coplanar waveguide feed integrated with the feed structure [6].

Yang Xiao et al. [2] proposed a multiband, low-profile wearable antenna using a Graphene assembled film AMC to reduce SAR and body coupling. It was designed to operate at 3 bands with peak gain up to 7.9 dBi and SAR value within 0.51–0.61 W/kg across the bands. Yan et al. [15] developed a ‘low-profile dual-band textile antenna’ loaded with a 4×4 AMC array operating at 2.4 GHz and 5.15 GHz bands with return loss below -10 dB and gain of 2.5 dBi at 2.45 GHz and 4 dBi at higher band. Rouzegar et al. [16] proposed a wideband uniplanar AMC with curved microstrip line resonators. Current loops are used to improve bandwidth adaptability at different frequencies, such as 8.81 GHz and 12.23 GHz, with an antenna gain of 3.2 dBi.

Yao et al. [17] designed a broadband AMC chessboard for radar cross-section reduction to achieve wideband performance (12.1–20.5 GHz). He achieved antenna bandwidth of 14.3–17.2 GHz with 1.7 dB gain. Yang et al. [18] introduced a high-gain millimeter-wave LTCC antenna array with AMC backing. AMC properties were modeled using HFSS with a Floquet port. 6×6 AMC array is used to improve radiation efficiency, bandwidth and gain. Liu et al. [19] proposed a windmill-like broadband antenna with AMC for wearable off-body communication operating at 2.45 GHz and 5 GHz with a peak gain of 5.8 dBi. AMC enables close-to-skin low-profile operation while reducing SAR. Zhu et al. [20] developed a wideband, low-profile MIMO antenna with high isolation using 5×5 AMC unit cells. Bowtie dipole with V-shaped patches was used to operate the antenna at dual modes (3.5 and 4.5 GHz). He achieved port isolation below -25 dB.

3. Materials and Methods

The proposed antenna features a microstrip line-fed rectangular patch on a denim substrate with a relative permittivity 1.7. A human phantom model was incorporated to assess SAR compliance. The patch and feed structure were optimized to achieve resonance at 8.91 GHz with minimal backward radiation. The antenna's ground plane, substrate

thickness, and patch geometry were carefully chosen to enhance efficiency while ensuring mechanical flexibility for wearable applications.

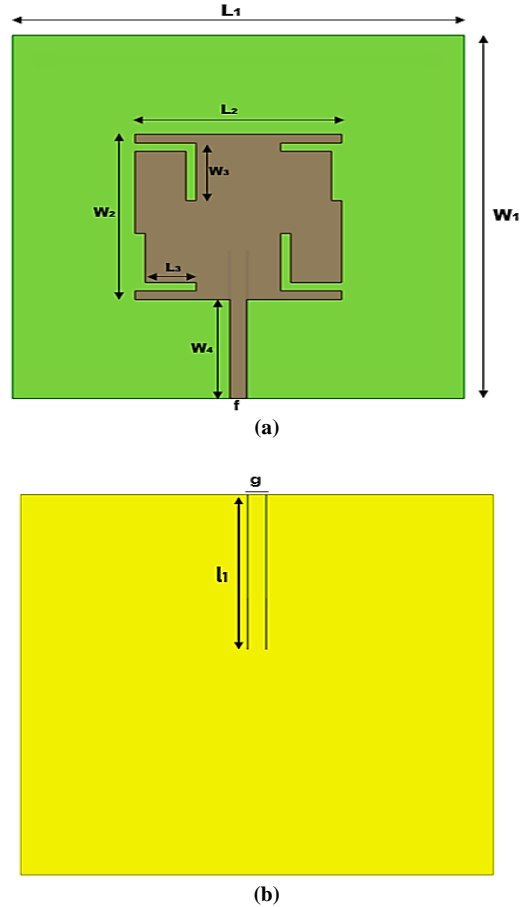


Fig. 1 (a) Top view of the antenna, and (b) Ground plane.

Table 1. Parameters of the antenna

Parameters	L ₁	L ₂	L ₃	W ₁	W ₂
Values in mm	66.4	30.4	7.5	66.4	30.2
Parameters	W ₃	W ₄	l ₁	g	f
Values in mm	10.5	18.1	27	2.8	2.4

Figure 1 depicts both the antenna's top layout and its ground-plane configuration. The WLF_MPA antenna is designed on a square substrate of 66.4 x 66.4 mm dimensions, which is of jean material that has a relative permittivity of 1.7, which is very low and suitable for wearable applications and loss tangent of 0.025 and a thickness of the jean material is 3mm. A shield is a super-electronic patch used as patch material for the wearable antenna. A rectangular patch is designed first and two “T”s are added. The total length and width of the patch are given as 30.4 mm and 30.3 mm. The length of the feed line is given as 27 mm. Full ground structures are employed in the antenna as there is no need for any more enhancement of the bandwidth and radiation efficiency. The dimensions of the designed antenna are listed in Table 1. The design equations are given as,

$$Width = a = \frac{\lambda}{2} \sqrt{\frac{2}{\epsilon_s + 1}} \quad (1)$$

$$\epsilon_{eff} = \frac{\epsilon_s + 1}{2} + \frac{\epsilon_s - 1}{2} \left(1 + \frac{12H}{a}\right)^{-1/2} \quad (2)$$

$$\Delta L = 0.412H \frac{(\epsilon_{eff} + 0.3) \left(\frac{a}{H} + 0.264\right)}{(\epsilon_{eff} + 0.258) \left(\frac{a}{H} + 0.264\right)} \quad (3)$$

$$L_S = 6H + L \quad W_S = 6H + a \quad (4)$$

4. Results and Discussion

This section presents the performance of the proposed wearable antenna, which resonates at 8.91 GHz and covers 8.72–9.09 GHz. Return-loss, VSWR characteristics, along with gain and directivity performance measures, have been used to evaluate the performance of the proposed antenna. A specific absorption rate study is also included to confirm that the design meets safety limits for human exposure.

4.1. Return Loss and Impedance Matching

Figure 2 illustrates the $|S_{11}|$ response of the antenna, where $|S_{11}|$ falls below -10 dB from 8.72 GHz to 9.09 GHz, indicating efficient impedance matching and minimal reflection of power. A lower return loss ensures that most of the input power is transmitted, enhancing overall antenna performance.

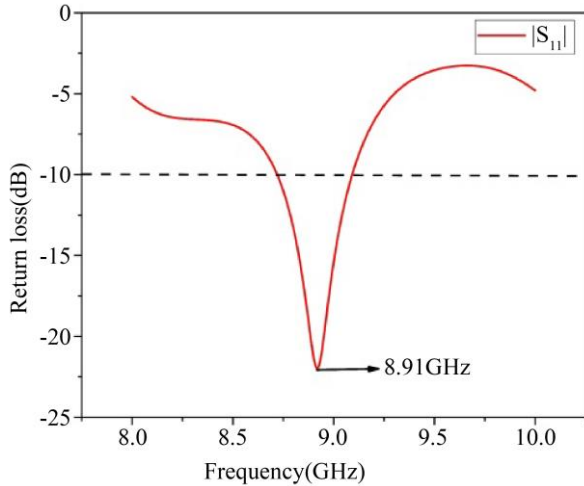


Fig. 2 Return loss of the simulated antenna

4.2. VSWR and Transmission Efficiency

Figure 3 presents the Vertical Standing Wave Ratio (VSWR), which remains between 1 and 2 across the working band. A VSWR closer to 1 indicates better power transmission, minimizing signal loss and ensuring stable communication in wearable applications.

4.3. Gain and Directivity Analysis

The measured peak gain of 6.4 dB signifies the antenna’s ability to efficiently radiate power in the intended direction,

while the peak gain of 4.052 dB suggests a balance between omnidirectional and directional radiation characteristics. This makes the antenna suitable for dynamic on-body applications, where consistent signal strength is crucial.

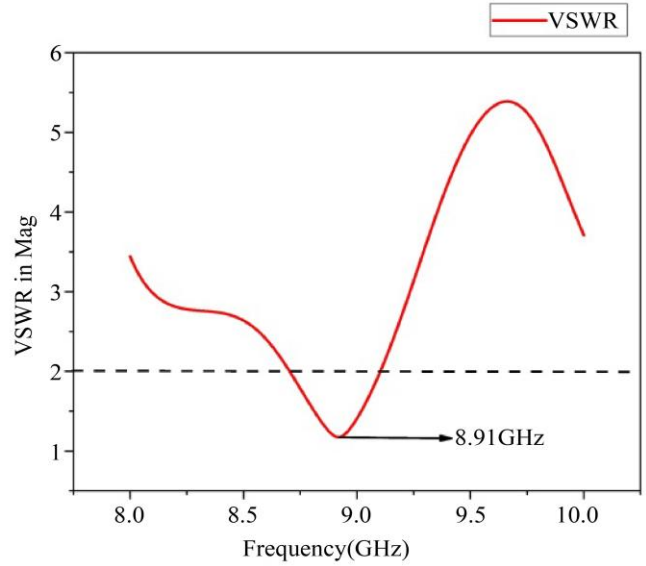


Fig. 3 VSWR of the simulated antenna

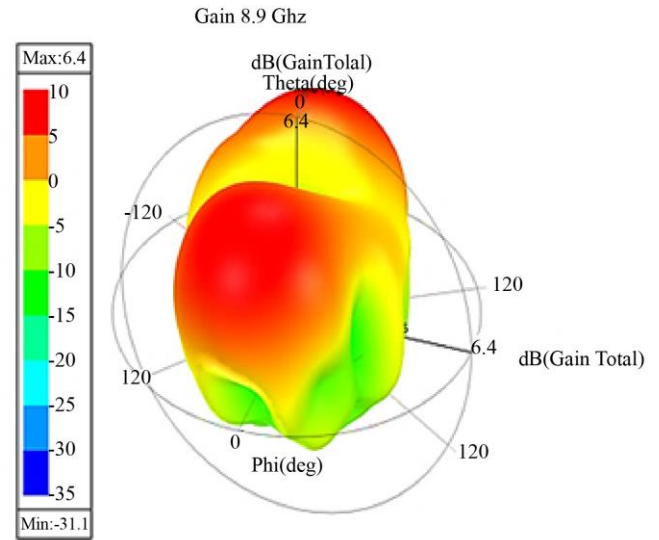


Fig. 4 Gain plot of the antenna

4.4. Front-to-Back Ratio

The high front-to-back ratio of 49.51 dB exceeds the standard threshold for wearable antennas, ensuring minimal radiation exposure towards the body and enhancing efficiency. This is particularly important for health and safety compliance in wearable technology.

4.5. Surface Current Distribution

Figure 5 illustrates the surface current distribution, highlighting the antenna’s radiation efficiency and interaction with different layers of the wearable environment.

Proper current distribution across the patch ensures stable performance, reduced power losses, and enhanced antenna effectiveness in real-world applications.

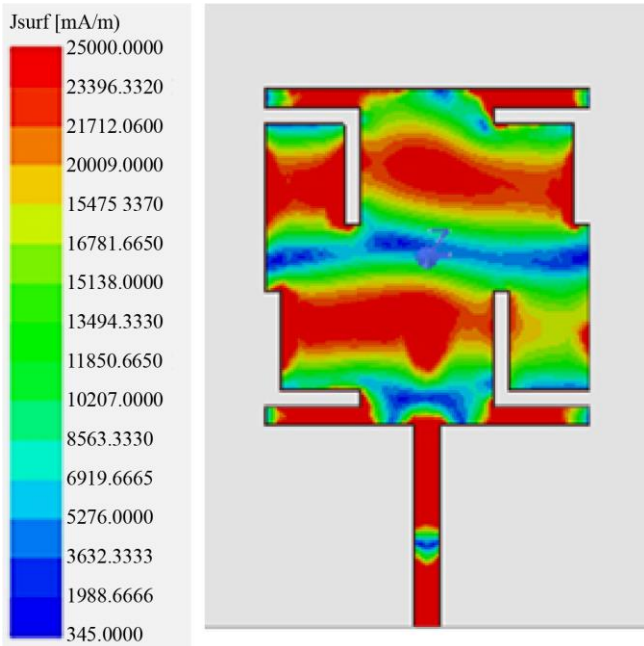


Fig. 5 Surface current distribution of the antenna

4.6. Human Tissue Model and SAR Analysis

Figure 6 depicts the antenna’s E- and H-plane radiation patterns, highlighting its directivity. Figure 7 illustrates the three-layer human-tissue phantom used for SAR evaluation—skin, fat, and muscle. The dielectric properties assigned are: skin ($\epsilon_r = 33.18$, $\tan \delta = 0.39$), fat ($\epsilon_r = 4.14$, $\tan \delta = 0.32$), and muscle ($\epsilon_r = 45.5$, $\tan \delta = 0.38$) [1].

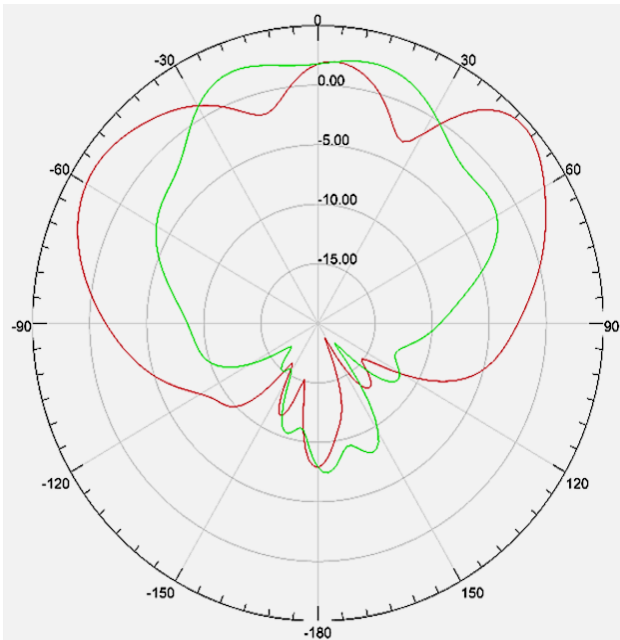


Fig. 6 Radiation pattern of the antenna

Figure 8 illustrates the SAR distribution for the proposed antenna, with a maximum localized SAR of 0.8912 W/kg—well under the 1.6 W/kg threshold specified by ANSI for 1 g of tissue. To obtain these values, a three-layer human phantom (skin, fat, muscle) was modelled in ANSYS HFSS. The computed average SAR over 1 g of muscle tissue is 1.6 W/kg, which also lies below the 2 W/kg international safety ceiling. These low SAR metrics confirm the antenna design is safe for wearable use without compromising on-body communication performance.

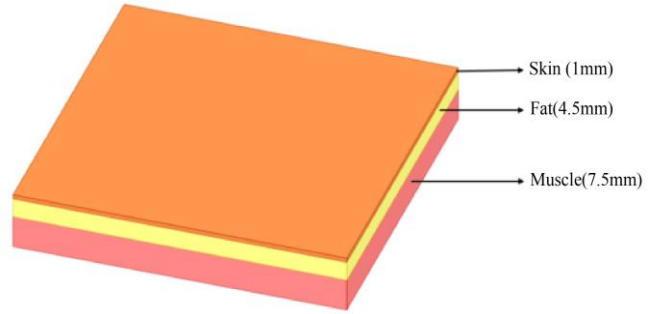


Fig. 7 Model of human phantom

Table 2. Antenna performance measures

Parameter	Value
Peak gain	6.4dB
Peak directivity	3.153
Front-to-back ratio	33.82
Antenna efficiency	72.39%

The antenna performance measures are given in Table 2. The antenna has a front-to-back ratio of 33.82, above 26 [5], which is suitable for wearable antennas. Other parameters, such as peak gain, directivity and antenna efficiency, are also discussed.

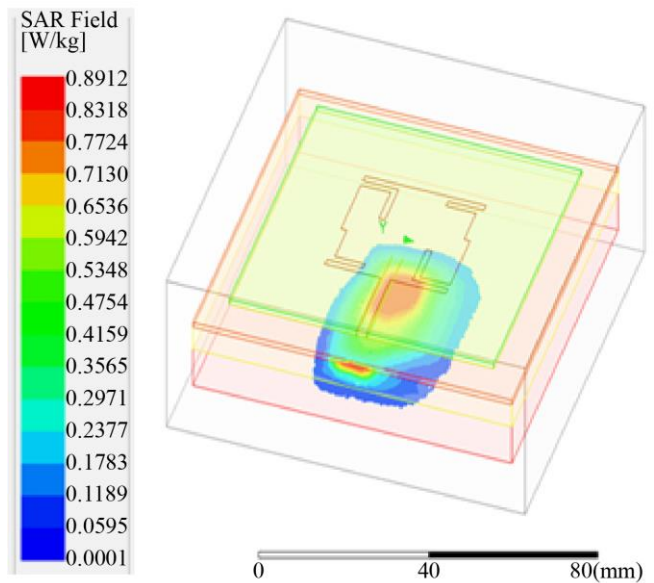


Fig. 8 SAR distribution of the antenna

4.7. State of Art Comparison

Compared to previously reported wearable antennas, the proposed WLF_MPA demonstrates a balanced combination of high performance, flexibility, and cost-effectiveness. Table 3 compares the proposed method with other state-of-the-art methods. While Çelenk et al. [1] and Muthu Krishnan [5] utilized expensive textile structures and complex SIW techniques, the proposed design achieves a comparable gain of 6.4 dB and an antenna efficiency of 72.39% using low-cost denim material. Unlike Xiao et al. [2], who reported excellent flexibility but required advanced GAF and PDMS

fabrication, but the designed antenna denim-based antenna offers good flexibility and robustness without the need for specialized materials. Furthermore, the SAR value (0.8912 W/kg) remains comfortably below safety limits, similar to the best values reported in the literature but achieved here with a simpler and cheaper setup. The high front-to-back ratio of 33.82 dB exceeds typical thresholds for wearable designs, ensuring reduced back radiation towards the body. Overall, the proposed antenna presents a favourable trade-off between performance, safety, durability, and affordability, making it highly suitable for scalable wearable applications.

Table 3. Comparison with other methods

Feature	Çelenk et al. [1]	Xiao et al. [2]	Potey [3]	Muthu Krishnan [5]	Proposed Method
Main Material	Textile with SIW structure	Graphene Assembled Film (GAF) + PDMS	Cotton, Polyester, Lycra, Cordura	Textile with SIW cavity	Denim fabric substrate
Operating Frequency	8 GHz (X-band)	2.26–2.46 GHz, 3.52–3.68 GHz, 4.94–5.26 GHz	2.45 GHz	5.8 GHz	8.72–9.09 GHz (centered at 8.91 GHz)
Bandwidth	26%	Covers WiFi, 5G n77, 5G WLAN bands	Depends on fabric (Return Loss based)	4.8% impedance BW, 2.9% axial ratio BW	370 MHz bandwidth (~4.16%)
Peak Gain	5.2 dBi	5.7–7.9 dBi	Cotton: 3.8 dBi, Polyester: 6.8 dBi, Cordura: 5.9 dBi, Lycra: 6.8 dBi	5 dBi	6.4 dB
Efficiency	79.2%	Not directly given (focus on SAR and gain)	Cotton: 35%, Polyester: 76%, Cordura: 64%, Lycra: 67%	Not explicitly mentioned	70%
SAR (Specific Absorption Rate)	0.53–0.69 W/kg (10g tissue, 30 dBm)	0.51 W/kg @2.36GHz, 0.61 W/kg @3.6GHz, 0.562 W/kg @5.1GHz (1g tissue)	Not reported	<1.27 W/kg (1W source, 1g tissue)	0.8912 W/kg (1g muscle tissue)
Flexibility & Conformability	Good underbending (on body)	Excellent (GAF and PDMS combination)	Depends on fabric flexibility	Good, tested on curved surfaces	Good flexibility; comfortable and durable with denim
Polarization	Linear	Linear	Linear	Dual-sense Circular (RHCP & LHCP)	Linear polarization
Fabrication Method	Standard textile techniques, off-the-shelf parts	Flexible material layering	Textile patch with IE3D simulation	SIW cavity integration with textile	Simple microstrip-fed patch fabrication using denim
Special Feature	Military badge design, Aircraft shape, mass production friendly	Multiband operation with low SAR	Comparison of fabric substrates	Switchable circular polarization by changing feed	Low-cost, wearable, SAR-compliant antenna for industrial, healthcare, and defense

5. Conclusion

The use of jean substrate as a replacement for costly textile fabric and conductive copper patch, respectively, demonstrates a cost-effective approach to designing wearable antennas. The antenna exhibits excellent performance with $|S_{11}|$ below -10dB and VSWR across the entire X-Band frequency range, making it suitable for various applications,

including weather monitoring, industrial health monitoring, and military applications. With a resonant frequency of 8.70 GHz and a measured gain of 5.6dB at 8.7GHz, the antenna offers reliable performance. Additionally, its low Specific Absorption Rate value of 0.8912W/Kg for 1g muscle mass ensures compliance with safety standards, further enhancing its suitability for wearable applications.

References

- [1] Esra Çelenk, and Nurhan Türker Tokan, "All-Textile On-Body Antenna for Military Applications," *IEEE Antennas and Wireless Propagation Letters*, vol. 21, no. 5, pp. 1065-1069, 2022. [[CrossRef](#)] [[Google Scholar](#)] [[Publisher Link](#)]
- [2] Yang Xiao et al., "Multiband and Low-Specific-Absorption-Rate Wearable Antenna with Low Profile Based on Highly Conductive Graphene Assembled Film," *IEEE Antennas and Wireless Propagation Letters*, vol. 22, no. 9, pp. 2195-2199, 2023. [[CrossRef](#)] [[Google Scholar](#)] [[Publisher Link](#)]
- [3] Pranita Manish Potey, and Kushal Tuckley, "Design of Wearable Textile Antenna with Various Substrate and Investigation on Fabric Selection," *2018 3rd International Conference on Microwave and Photonics (ICMAP)*, Dhanbad, India, pp. 1-2, 2018. [[CrossRef](#)] [[Google Scholar](#)] [[Publisher Link](#)]
- [4] T. Yorozu et al., "Electron Spectroscopy Studies on Magneto-Optical Media and Plastic Substrate Interface," *IEEE Translation Journal on Magnetics in Japan*, vol. 2, no. 8, pp. 740-741, 1987. [[CrossRef](#)] [[Google Scholar](#)] [[Publisher Link](#)]
- [5] R. Muthu Krishnan, and G. Kannan, "A Compact Dual-Sense Circularly Polarized SIW Textile Antenna for Body-Centric Wireless Communication," *AEU - International Journal of Electronics and Communications*, vol. 160, 2023. [[CrossRef](#)] [[Google Scholar](#)] [[Publisher Link](#)]
- [6] Huachong Liu et al., "A CPW-FED Dual-Band Dual-Pattern Radiation Patch Antenna Based on TM01 and TM02 Mode," *2020 9th Asia-Pacific Conference on Antennas and Propagation (APCAP)*, Xiamen, China, pp. 1-2, 2020. [[CrossRef](#)] [[Google Scholar](#)] [[Publisher Link](#)]
- [7] Muhammad Azfar bin Abdullah et al., "Integrated Two Textile Dipole Antenna with Dual-Band Textile Artificial Magnetic Conductor," *2013 7th European Conference on Antennas and Propagation (EuCAP)*, Gothenburg, Sweden, pp. 2075-2078, 2013. [[Google Scholar](#)] [[Publisher Link](#)]
- [8] Łukasz Januszkiwicz et al., "The Analysis of Influence of Textile Antenna Location on its Performance," *2015 9th European Conference on Antennas and Propagation (EuCAP)*, Lisbon, Portugal, pp. 1-5, 2015. [[Google Scholar](#)] [[Publisher Link](#)]
- [9] Eva Rajo-Iglesias et al., "Textile Soft Surface for Back Radiation Reduction in Bent Wearable Antennas," *IEEE Transactions on Antennas and Propagation*, vol. 62, no. 7, pp. 3873-3878, 2014. [[CrossRef](#)] [[Google Scholar](#)] [[Publisher Link](#)]
- [10] Ezzaty Faridah Nor Mohd Hussin et al., "A Wearable Textile Dipole for Search and Rescue Application," *2016 5th International Conference on Electronic Devices, Systems and Applications (ICEDSA)*, Ras Al Khaimah, United Arab Emirates, pp. 1-4, 2016. [[CrossRef](#)] [[Google Scholar](#)] [[Publisher Link](#)]
- [11] Nacer Chahat, Maxim Zhadobov, and Ronan Sauleau, "Wearable Textile Patch Antenna for BAN At 60 GHz," *2013 7th European Conference on Antennas and Propagation (EuCAP)*, Gothenburg, Sweden, pp. 217-219, 2013. [[Google Scholar](#)] [[Publisher Link](#)]
- [12] Tero Kaija, Juha Lilja, and Pekka Salonen, "Textile Antennas: Shotgun Proven Performance," *2011 - MILCOM 2011 Military Communications Conference*, Baltimore, MD, USA, pp. 459-464, 2011. [[CrossRef](#)] [[Google Scholar](#)] [[Publisher Link](#)]
- [13] Jan Špůrek et al., "Slot Loop Antennas Printed on 3D Textile Substrate," *2016 21st International Conference on Microwave, Radar and Wireless Communications (MIKON)*, Krakow, Poland, pp. 1-3, 2016. [[CrossRef](#)] [[Google Scholar](#)] [[Publisher Link](#)]
- [14] Mai A.R. Osman et al., "Design and Analysis UWB Wearable Textile Antenna," *Proceedings of the 5th European Conference on Antennas and Propagation (EUCAP)*, Rome, Italy, pp. 530-533, 2011. [[Google Scholar](#)] [[Publisher Link](#)]
- [15] Sen Yan, Ping Jack Soh, and Guy A.E. Vandenbosch, "Low-Profile Dual-Band Textile Antenna with Artificial Magnetic Conductor Plane," *IEEE Transactions on Antennas and Propagation*, vol. 62, no. 12, pp. 6487-6490, 2014. [[CrossRef](#)] [[Google Scholar](#)] [[Publisher Link](#)]
- [16] Seyed Mohammadreza Rouzegar, Abbas Alighanbari, and Omar M. Ramahi, "Wideband Uniplanar Artificial Magnetic Conductors Based on Curved Coupled Microstrip Line Resonators," *IEEE Microwave and Wireless Components Letters*, vol. 27, no. 4, pp. 326-328, 2017. [[CrossRef](#)] [[Google Scholar](#)] [[Publisher Link](#)]
- [17] Pei Yao, Binzhen Zhang, and Junping Duan, "A Broadband Artificial Magnetic Conductor Reflecting Screen and Application in Microstrip Antenna for Radar Cross-Section Reduction," *IEEE Antennas and Wireless Propagation Letters*, vol. 17, no. 3, pp. 405-409, 2018. [[CrossRef](#)] [[Google Scholar](#)] [[Publisher Link](#)]
- [18] W.C. Yang et al., "High-Gain and Low-Loss Millimeter-Wave LTCC Antenna Array Using Artificial Magnetic Conductor Structure," *IEEE Transactions on Antennas and Propagation*, vol. 63, no. 1, pp. 390-395, 2015. [[CrossRef](#)] [[Google Scholar](#)] [[Publisher Link](#)]

- [19] XiongYing Liu et al., "A Planar Windmill-Like Broadband Antenna Equipped with Artificial Magnetic Conductor for Off-Body Communications," *IEEE Antennas and Wireless Propagation Letters*, vol. 15, pp. 64-67, 2016. [[CrossRef](#)] [[Google Scholar](#)] [[Publisher Link](#)]
- [20] Jianfeng Zhu et al., "Wideband Low-Profile Highly Isolated MIMO Antenna with Artificial Magnetic Conductor," *IEEE Antennas and Wireless Propagation Letters*, vol. 17, no. 3, pp. 458-462, 2018. [[CrossRef](#)] [[Google Scholar](#)] [[Publisher Link](#)]